

An Artificial Receptor for Dimethyl Aspartate

Tadashi Mizutani,* Takeshi Murakami, Takuya Kurahashi, and Hisanobu Ogoshi*

Department of Synthetic Chemistry and Biological Chemistry, Faculty of Engineering, Kyoto University,
Yoshida, Sakyo-ku, Kyoto 606-01, Japan

Received March 23, 1995 (Revised Manuscript Received August 18, 1995²)

[*trans*-5,15-Bis(2,7-dihydroxy-1-naphthyl)-2,3,7,8,12,13,17,18-octaethylporphyrinato]zinc(II) (**1**), a trifunctionalized porphyrin host, was prepared as a receptor for amino acid derivatives, particularly those having a hydrogen-bonding site in the side chain. The free energy changes for the binding of Leu-OMe, Asp-OMe, and Glu-OMe to **1** were -5.8 kcal/mol, -6.6 kcal/mol, and -5.9 kcal/mol, showing a selectivity for Asp-OMe. ¹H NMR titration experiments indicated that three simultaneous attractive interactions, one coordination interaction, and two hydrogen-bonding interactions, are operating in the host–guest complex. The preference for Asp-OMe over Glu-OMe was found to originate from the favorable enthalpy term for Asp-OMe. The free energy change, the enthalpy change, and the entropy change were determined and split into contributions arising from coordination interaction and from hydrogen-bonding interactions by use of reference hosts. Comparison of enthalpy and entropy changes suggests that the host–guest complex becomes more ordered as the number of recognition pairs increases.

Mechanism of selectivity of molecular recognition of biologically active molecules, especially of flexible guest molecules, is interesting since several factors are competitively contributing to the thermodynamics of the recognition process. Elementary processes such as attractive forces between the host and the guest, conformational changes in host and guest, and solvation state changes during the host–guest complex formation all make important contributions to the recognition process. Entropic contribution owing to the restriction of motion upon complexation is also important for a flexible guest.¹ Evaluation of each recognition interaction by use of reference host and guest has been proved to be helpful in understanding multipoint host–guest complexation as exemplified by several previous papers.^{2,3} Thermodynamic parameters (ΔG° , ΔH° , and ΔS°) for molecular recognition have been studied for many host–guest systems.⁴ It should be noted that the values of ΔG° , ΔH° , and ΔS° for the overall process involve contributions from many elementary processes, so a unifying interpretation

is difficult to make.⁵ By using less polar solvents, we can reduce the solvation interaction to minimal and focus on the host–guest interaction.⁶ Under these conditions, the entropy changes (ΔS°) directly reflect the changes in motion of the host–guest molecules. We can estimate how effectively the certain host–guest interaction induces the ordered state in the host–guest complex by monitoring entropy changes.

Intermolecular interaction within the host–guest complex can be classified into two categories. The first one is the interaction between some specific groups, which may be called point–point interaction or point recognition. The second one is the interaction between the whole molecules such as charge transfer interaction between the HOMO of a molecule and the LUMO of another and hydrophobic interaction. This can be called surface–surface interaction. We focus on point–point interactions in the present paper. We regard the overall host–guest interaction as being equal to the sum of the interaction between functional groups. The free energy changes, the enthalpy changes, and the entropy changes of the recognition process can be split into contributions arising from each pairing of recognition groups by assuming the hypothetical intermediate thermodynamic states. These changes can be experimentally determined by use of reference host or reference guest.⁷

Studies of amino acid recognition have been carried out mostly for aromatic or hydrophobic amino acid derivatives.⁸ To our knowledge, studies of recognition of amino acid derivatives with polar side chains are rare.⁹ For recognition of such amino acids, at least three recognition groups are necessary. For effective interaction between functional groups, internal rotational freedom of the amino acid derivative should be frozen.

(5) Recently, interpretation of the thermodynamic data (ΔG° , ΔH° , and ΔS°) in terms of solvation term and conformational energy term is reported. see ref 4k.

(6) For importance of solvation energy, see: (a) Adrian, J. C., Jr.; Wilcox, C. S. *J. Am. Chem. Soc.* **1992**, *114*, 1398. (b) Carcanague, D. R.; Knobler, C. B.; Diederich, F. *J. Am. Chem. Soc.* **1992**, *114*, 1515. (c) Bonar-Law, R. P.; Sanders, J. K. M. *J. Am. Chem. Soc.* **1995**, *117*, 259. (d) Mizutani, T.; Murakami, T.; Matsumi, N.; Kurahashi, T.; Ogoshi, H. *J. Chem. Soc., Chem. Commun.* **1995**, 1257.

(7) Ogoshi, H.; Ema, T.; Kato, Y.; Mizutani, T.; Kuroda, Y. *Supramol. Chem.* **1995**, *6*, 115.

* Abstract published in *Advance ACS Abstracts*, December 15, 1995.

(1) Mizutani, T.; Ema, T.; Ogoshi, H. *Tetrahedron* **1995**, *51*, 473.
(2) (a) Aoyama, Y.; Asakawa, M.; Yamagishi, A.; Toi, H.; Ogoshi, H. *J. Am. Chem. Soc.* **1990**, *112*, 3145. (b) Aoyama, Y.; Asakawa, M.; Matsui, Y.; Ogoshi, H. *J. Am. Chem. Soc.* **1991**, *113*, 6233. (c) Hayashi, T.; Miyahara, T.; Hashizume, N.; Ogoshi, H. *J. Am. Chem. Soc.* **1993**, *115*, 2049. (d) Mizutani, T.; Ema, T.; Yoshida, T.; Kuroda, Y.; Ogoshi, H. *Inorg. Chem.* **1993**, *32*, 2072. (e) Mizutani, T.; Ema, T.; Tomita, T.; Kuroda, Y.; Ogoshi, H. *J. Am. Chem. Soc.* **1994**, *116*, 4240. (f) Hayashi, T.; Miyahara, T.; Aoyama, Y.; Nonoguchi, M.; Ogoshi, H. *Chem. Lett.* **1994**, 1749.

(3) Schneider, H.-J.; Shiestel, T.; Zimmermann, P. *J. Am. Chem. Soc.* **1992**, *114*, 7698.

(4) (a) Canceill, J.; Lacombe, L.; Collet, A. *C.R. Hebd. Seances Acad. Sci., Ser. 2* **1987**, *304*, 815. (b) Tabushi, I.; Mizutani, T. *Tetrahedron* **1987**, *43*, 1439. (c) Williams, K.; Askew, B.; Ballester, P.; Buhr, C.; Jeong, K. S.; Jones, S.; Rebek, J., Jr. *J. Am. Chem. Soc.* **1989**, *111*, 1090. (d) Stauffer, D. A.; Barrans, R. E., Jr.; Dougherty, D. A. *J. Org. Chem.* **1990**, *55*, 2762. (e) Harvey, N. G.; Rose, P. L.; Mirajovsky, D.; Arnett, E. *J. Am. Chem. Soc.* **1990**, *112*, 3547. (f) Mazor, M. H.; McCammon, J. A.; Lybrand, T. P. *J. Am. Chem. Soc.* **1990**, *112*, 4411. (g) Adrian, J. C., Jr.; Wilcox, C. S. *J. Am. Chem. Soc.* **1991**, *113*, 678. (h) Smithrud, D. B.; Sanford, E. M.; Chao, I.; Ferguson, S. B.; Carcanague, D. R.; Evanseck, J. D.; Houk, K. N.; Diederich, F. *Pure Appl. Chem.* **1990**, *62*, 2227. (i) Cox, J. P. L.; Nicholls, I. A.; Williams, D. H. *J. Chem. Soc., Chem. Commun.* **1991**, 1295. (j) Diederich, F.; Smithrud, D. B.; Sanford, E. M.; Wyman, T. B.; Ferguson, S. B.; Carcanague, D. R.; Chao, I.; Houk, K. N. *Acta Chem. Scand.* **1992**, *46*, 205. (k) Inoue, Y.; Hakushi, T.; Liu, Y.; Tong, L.; Shen, B.; Jin, D. *J. Am. Chem. Soc.* **1993**, *115*, 475.

Compensation of ΔH and ΔS is expected for such a process. Rizzarelli and co-workers^{9a} reported that histidine forms a more stable complex than does histamine with Cu^{2+} with an additional AlaO^- ligand in water. The stronger binding of histidine over histamine is entropy driven. Because the complexation experiments of Rizzarelli were carried out in water, the enthalpy term and the entropy term should be much affected by the solvation state changes. Other interactions such as conformation energy, hydrogen-bonding energy, and coordination energy are thus in some cases difficult to observe in water. To probe these interactions, use of organic solvent is advantageous.

In the present paper, we report the preparation of a trifunctional porphyrin host as a model receptor for dimethyl aspartate and the comparative studies of the binding of amino acid derivatives by the trifunctional as well as difunctional and monofunctional porphyrin hosts. The binding studies were performed in chloroform to minimize the contribution from solvation effects to the thermodynamic parameters.

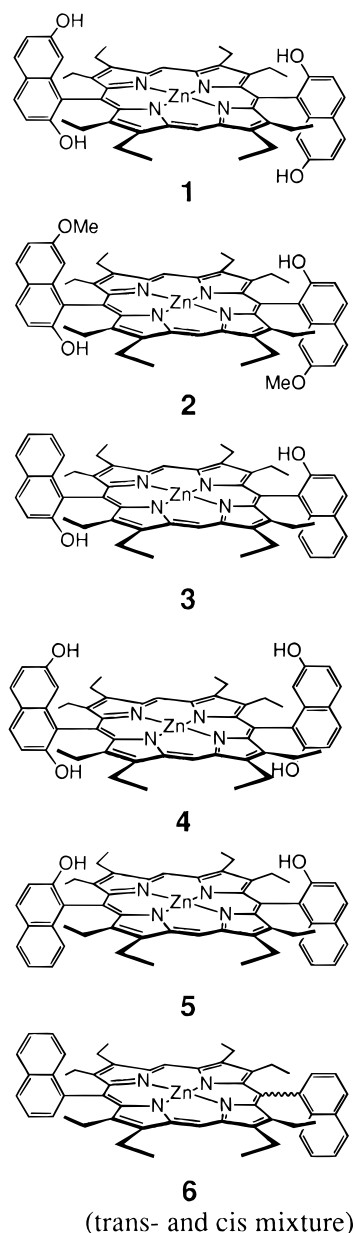
Results

Preparation of Trifunctional Porphyrin Host 1.

[*trans*-5,15-Bis(2,7-dihydroxy-1-naphthyl)-2,3,7,8,12,13,17,18-octaethylporphyrinato]zinc(II) (**1**) (Chart 1) was prepared by condensation of 3,3',4,4'-tetraethyl-2,2'-dipyrrylmethane with 2-hydroxy-7-methoxy-1-naphthaldehyde (Scheme 1). The precursor aldehyde **12** was prepared from 2,7-dihydroxynaphthalene, by protecting the two hydroxyl groups with methyl iodide, followed by formylation by Vilsmeier reaction and the selective deprotection of the 2-hydroxyl group with BBr_3 . As a direct approach, 2,7-dihydroxy-1-naphthaldehyde was first condensed with the dipyrromethane to give 5,15-bis(2,7-dihydroxy-1-naphthyl)-2,3,7,8,12,13,17,18-octaethylporphyrin (**15** and *cis* isomer of **15**). Separation of the *trans* isomer from the *cis* isomer, however, was unsuccessful with this compound. Therefore we prepared 5,15-bis(2-hydroxy-7-methoxy-1-naphthyl)-2,3,7,8,12,13,17,18-octaethylporphyrin (**13** and **14**) first. With these porphyrins, the *trans* isomer was easily separated from the *cis* isomer by column chromatography. The methoxy group was then deprotected by BBr_3 , and zinc was inserted in a usual manner to yield **1**. The structure of the *cis* isomer **13** was confirmed by reacting it with 1,8-dibromooctane in $\text{K}_2\text{CO}_3/\text{acetone}$ to yield the bridged porphyrin **16** (Scheme 2). The bridged porphyrin **16** was identified by the $^1\text{H}-^1\text{H}$ COSY and FAB-mass spectroscopy.

Host **1** has C_{2h} symmetry, and owing to this symmetry, two identical coordination sites exist. Host **1** has a zinc ion and two hydroxyl groups in a binding pocket. Because only 1:1 complexation is known for zinc porphy-

Chart 1



rins,¹⁰ we expect that host **1** shows only one binding constant. Host **3** is a reference host, which lacks a pair of 7-hydroxyl groups on the naphthyl rings. The *cis* isomers of these hosts, host **4** and host **5**, also serve as trifunctional hosts. Lack of the symmetry, however, results in the two different coordination sites, and we expect to obtain two binding constants for **4** and **5**.

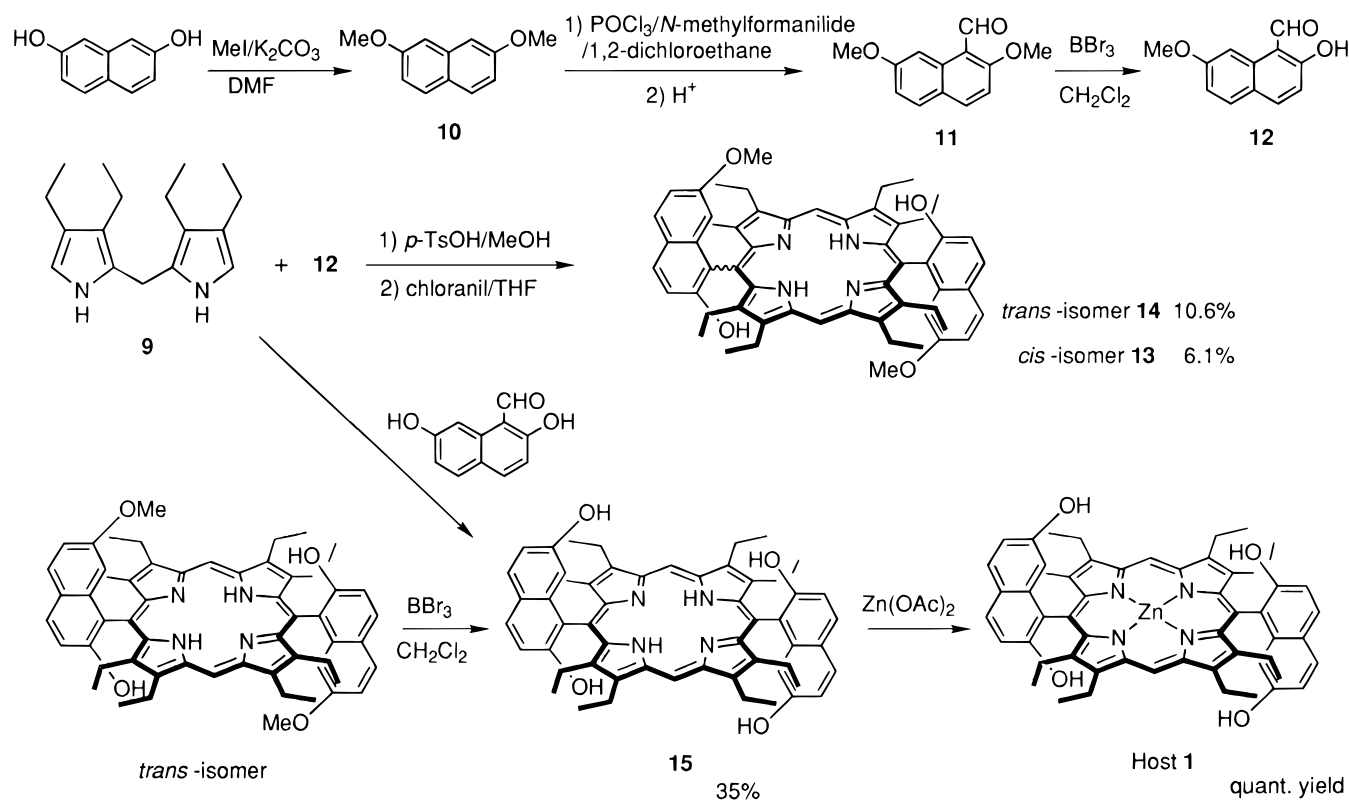
Determination of the Binding Constants between α -Amino Acid Esters and Porphyrin Hosts. The binding constants between amino acid esters and host **1** were determined by following the absorbance changes in the Soret band of **1** upon the addition of the guest molecules. The guest molecules used were leucine methyl ester (Leu-OMe), valine methyl ester (Val-OMe), alanine methyl ester (Ala-OMe), tryptophan methyl ester (Trp-OMe), aspartic acid dimethyl ester (Asp-OMe), glutamic acid dimethyl ester (Glu-OMe), proline methyl ester (Pro-OMe), cysteine methyl ester (Cys-OMe), and methionine methyl ester (Met-OMe). All these amino

(8) (a) Rebek, J., Jr.; Nemeth, D. *J. Am. Chem. Soc.* **1985**, *107*, 6738. (b) Nakagawa, T.; Shibukawa, A.; Kaihara, A.; Itamochi, T.; Tanaka, H. *J. Chromatogr.* **1986**, *353*, 399. (c) Pirkle, W. H.; Pochapsky, T. C. *J. Am. Chem. Soc.* **1987**, *109*, 5975. (d) Andersson, L. I.; O'Shannessy, D. J.; Mosbach, K. *J. Chromatogr.* **1990**, *513*, 167. (e) Murakami, Y.; Ohno, T.; Hayashida, O.; Hisaeda, Y. *J. Chem. Soc., Chem. Commun.* **1991**, 950. (f) Galan, A.; Andreu, D.; Echavarren, A. M.; Prados, P.; de Mendoza, J. *J. Am. Chem. Soc.* **1992**, *114*, 1511. (g) Kuroda, Y.; Kato, Y.; Higashioji, T.; Ogoshi, H. *Angew. Chem.* **1993**, *105*, 774.

(9) (a) Borghesani, G.; Pulidori, F.; Remelli, M.; Purrello, R.; Rizzarelli, E. *J. Chem. Soc., Dalton Trans.* **1990**, 2095. (b) Ikeura, Y.; Kurihara, K.; Kunitake, T. *J. Am. Chem. Soc.* **1991**, *113*, 7342. (c) Heath, J. G.; Arnett, E. M. *J. Am. Chem. Soc.* **1992**, *114*, 4500. (d) Liu, R.; Still, W. C. *Tetrahedron Lett.* **1993**, *34*, 2573.

(10) (a) Miller, J. R.; Dorough, G. D. *J. Am. Chem. Soc.* **1952**, *74*, 3977. (b) Kirksey, C. H.; Hambright, P.; Storm, C. B. *Inorg. Chem.* **1969**, *8*, 2141.

Scheme 1



acid esters were L-isomers. The titration was carried out at 25 °C in CHCl_3 containing either 1% ethanol or, 0.1% amylene as a stabilizer or containing no stabilizer. Even a small amount of ethanol present in chloroform results in a reduced binding constant. This reduction in the binding constant is due to the interaction between ethanol and the recognition groups (Zn, C=O, and OH). UV-vis titration experiments were carried out both in 1%EtOH- CHCl_3 and in EtOH-free CHCl_3 . ^1H NMR and variable-temperature UV-vis titration experiments were carried out in EtOH-free CHCl_3 or CDCl_3 . The binding constants in amylene-containing chloroform agreed with those in pure chloroform within experimental errors.

In the UV-vis titration experiment, the absorbance at 414 nm increased and that at 428 nm decreased isospectically as the guest was added. The binding constants were determined by curve fitting to the absorbance changes at 414 and 428 nm on the assumption of a 1:1

complexation. The standard deviation of the binding constant was within 5%. The binding constants for host **3** were similarly determined. Host **6** is a mixture of *cis* and *trans* atropisomers, and the spectral changes upon guest addition were more complicated. At least three configurations are possible for this host: one configuration of a complex of *trans*-**6** and guest and two configurations of a complex of *cis*-**6** and guest depending on the coordination site occupied by the guest (Figure 1). Therefore only the absorbance change at 428 nm was used to determine a single binding constant, and the binding constant obtained should be regarded as a sum for those configurations. The binding constants are summarized in Table 1.

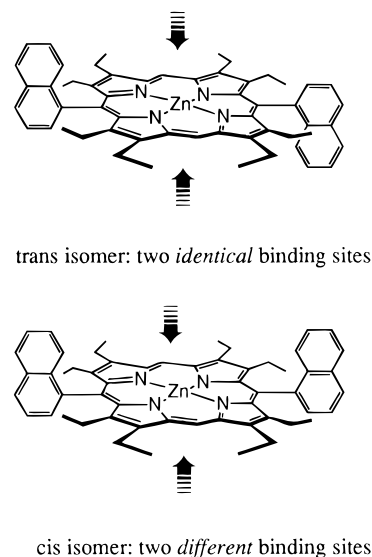
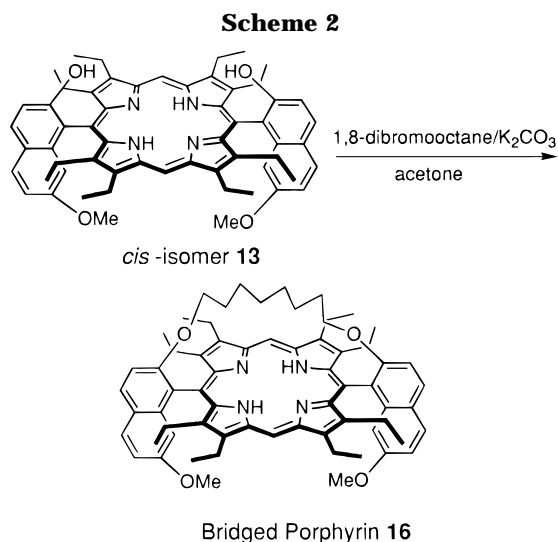


Figure 1. Binding site of porphyrin hosts. The *trans* isomer has only one kind of binding pocket, while the *cis* isomer has two binding pockets.

Table 1. Binding Constants (K , M^{-1}) between Hosts 1–3 and Amino Acid Esters in $CHCl_3$ (Either Containing 1% Ethanol or No Additive) at 25 °C

	$K(1)$	$K(2)$	$K(3)$	$K(1)/K(3)$	$K(2)/K(3)$	solvent ^a
Leu-OMe	7620	3310	6010	1.27	0.55	a
Val-OMe	7800	2460	4490	1.74	0.55	a
Ala-OMe	4010	1080	1490	2.69	0.72	a
Trp-OMe	18200	4140	5720	3.18	0.72	a
Asp-OMe	20900	960	1560	13.4	0.62	a
Glu-OMe	7820	480	890	8.77	0.54	a
Leu-OMe	17800		13200	1.35		b
Asp-OMe	69800		2850	24.5		b
Glu-OMe	24000		2420	9.92		b
Pro-OMe	69000					a
Cys-OMe	6470					a
Met-OMe	6340					a

^a a, $CHCl_3$ containing 1% ethanol; b, $CHCl_3$ free from ethanol.

Table 2. Comparison of Binding Constants (K , M^{-1}) of Asp-OMe by Three-Point Recognition Hosts in $CHCl_3$ Containing 1% Ethanol at 25 °C^a

binding sites		
$K(7OH,7OH,Zn)$	$K(7OH,2OH,Zn)$	$K(2OH,2OH,Zn)$
17 600	10 450	4300

^a The binding constants for each binding site were calculated from the following equations: $K(7OH,7OH,Zn) = K(4-Asp-OMe) - K(2OH,2OH,Zn)$, where $K(4-Asp-OMe) = 21\,900$ and $K(2OH,2OH,Zn) = 4300\,M^{-1}$. $K(7OH,2OH,Zn) = K(1-Asp-OMe)/2$, where $K(1-Asp-OMe) = 20\,900\,M^{-1}$. The value of $K(1-Asp-OMe)$ was divided by two, because host **1** has two identical binding sites. $K(2OH,2OH,Zn) = K(5-Asp-OMe) - K(6-Asp-OMe)/2$, where $K(6-Asp-OMe) = 310\,M^{-1}$.

Host **1** shows large binding constants for Pro-OMe, Asp-OMe, and Trp-OMe. The large binding constant observed for Pro-OMe can be ascribed to a strong basicity of the secondary amino group of Pro-OMe. The binding constants determined in ethanol-free chloroform were 2.3 to 3.3 times larger than those in 1% EtOH- $CHCl_3$. We expect that, in 1% EtOH- $CHCl_3$, the interaction of ethanol with the recognition groups (Zn, OH, and C=O) partly blocks the binding pocket. These ethanol molecules must be released to accommodate the guest. This energetically unfavorable process can account for the reduced binding constants observed in 1% EtOH- $CHCl_3$.

For comparison, the ratios of the binding constants $K(1)/K(3)$ and $K(2)/K(3)$ are also listed in Table 1. These ratios represent the effects of the 7-hydroxyl group of host **1** and the 7-methoxy group of host **2** on the binding, respectively. The binding constants of **1** are 24.5-fold and 9.9-fold larger than those of **3** for dimethyl aspartate (Asp-OMe) and dimethyl glutamate (Glu-OMe) guests, respectively, in ethanol-free chloroform, which can be ascribed to the effect of the 7-hydroxyl group. These results indicate that the hydrogen bonding to the 7-hydroxyl group results in the high selectivity of host **1** toward Asp-OMe and Glu-OMe. On the other hand, the 7-methoxy group acts as a repulsive site for all the guests as seen from the smaller ratio of $K(2)/K(3)$ than one.

The selectivity for Asp-OMe was compared between three-point recognition hosts **1**, **4**, and **5**, which have the hydroxyl groups at different distances from the porphyrin plane. The binding constants for each recognition site are summarized in Table 2. The binding constant was largest for the binding site having two distant OH groups (7-OH) and was smallest for that having two proximal OH (2-OH). The small binding constant for the 2OH-2OH-Zn binding pocket can be understood by the molecular modeling investigation. It was difficult to build a complex having simultaneous coordination and two

Table 3. Complexation-Induced Shift Observed in Host 1^a

	$\Delta\delta$ (ppm)		
	Leu-OMe	Asp-OMe	Glu-OMe
2-OH	0.57	0.95	0.67
7-OH	0.40	0.97	0.98
naphthyl 8-H	-0.05	-0.16	-0.09

^a 500 MHz 1H NMR was obtained in $CDCl_3$ at either 30 °C (Asp-OMe and Glu-OMe) or 40 °C (Leu-OMe), $[1] = 5.37 \times 10^{-5}$ to 1.86×10^{-4} M, $[guest] = 0 - (2.57 \times 10^{-3})$ M.

hydrogens bonding in this binding pocket because the geometry of the guest does not fit to the binding pocket. The difference between binding pockets of 7OH-7OH-Zn and 7OH-2OH-Zn is not clear. It may be attributable to the conformational energy of the bound guest.

1H NMR Studies of the Binding. The 1H NMR spectral changes of host **1** upon addition of Leu-OMe, Asp-OMe, and Glu-OMe were recorded in $CDCl_3$. The hydroxyl protons of host **1** gave two resolved signals at 5.20 and 4.17 ppm in $CDCl_3$. Both signals were shifted downfield and the naphthyl H-8 proton shifted upfield by adding the guest. These complexation-induced shifts (CIS) are shown in Figure 2 and Table 3. The curves in Figure 2 are drawn by a least-squares curve fitting to the following equation:

$$\delta = \frac{-\delta_0 g_0 + \delta_1 g_0 + \delta_0 h_0 + \delta_1 h_0 - \frac{\delta_0}{K} + \frac{\delta_1}{K}}{2h_0} + \frac{\delta_0 \sqrt{1 + 2g_0 K + 2h_0 K + g_0^2 K^2 - 2g_0 h_0 K^2 + h_0^2 K^2}}{2h_0 K} - \frac{\delta_1 \sqrt{1 + 2g_0 K + 2h_0 K + g_0^2 K^2 - 2g_0 h_0 K^2 + h_0^2 K^2}}{2h_0 K}$$

where δ is the chemical shift in the presence of g_0 M guest, δ_1 is the saturated value of the chemical shift at a high concentration of guest, h_0 is the concentration of the host, and K is the binding constant. The hydroxyl protons appearing at the lower field were assigned to the 2-OH proton, and those appearing at the higher field were assigned to the 7-OH proton, based on the fact that the chemical shift observed for the OH proton of host **2** is close to that which appears at the lower field in the spectra of **1**. This assignment was also supported by the isoshielding map prepared for the magnetic field produced by the ring current of a porphyrin ring. The isoshielding map predicts that the proton of 2-OH shows -1.5 to 0.8 ppm of anisotropic chemical shift according to the geometry of molecular modeling.¹¹ The uncertainty of the shift arises from free rotation along the C2-O2 bond. The proton of 7-OH shows 0.3 to 2.0 ppm chemical shift displacements. From the difference in the averages of these values, we predict that the 7-OH proton appears 1.5 ppm upfield relative to the 2-OH proton, in reasonable agreement with observation. The binding constants determined by the complexation-induced shifts are Leu-OMe $K = 14\,900$ (2-OH), 14 100 (7-OH), 17 700 (naphthyl, 8-H) at 40 °C, Asp-OMe $K = 27\,000$ (2-OH), 28 100 (7-OH), 33 300 (naphthyl, 8-H) at 30 °C, and Glu-OMe $K = 19\,000$ (2-OH), 13 400 (7-OH), 12 100 (naphthyl, 8-H)

(11) (a) Johnson, C. E. J.; Bovey, F. A. *J. Chem. Phys.* **1958**, *29*, 1012. (b) Ogoshi, H.; Setsune, J.; Omura, T.; Yoshida, Z. *J. Am. Chem. Soc.* **1975**, *97*, 6461.

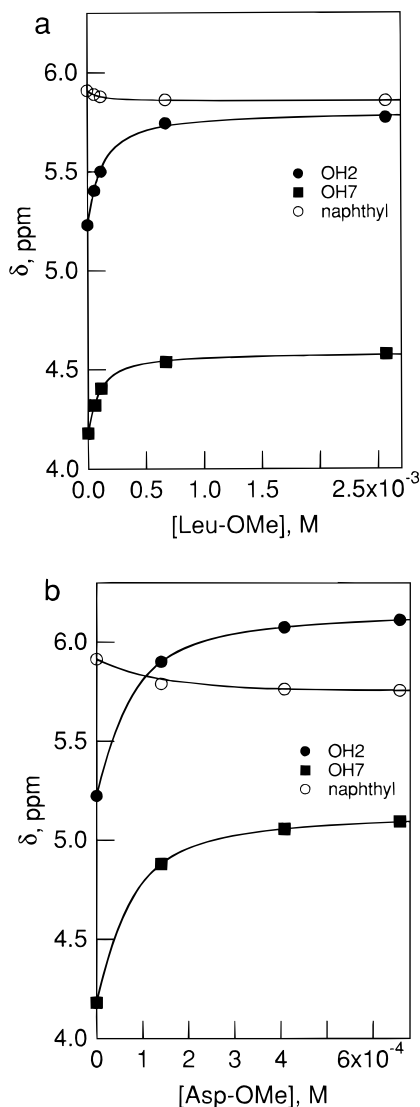


Figure 2. Chemical shift of host **1** induced by complexation with Leu-OMe (a) and Asp-OMe (b) in CDCl_3 . See also footnote of Table 3.

at 30 °C. In parentheses is shown the proton used for the determination of the binding constants.

Enthalpy and Entropy Changes in the Two-Point and Three-Point Recognition Host–Guest Systems.

Standard enthalpy (ΔH°) and standard entropy (ΔS°) changes of the binding were determined from the variable-temperature UV–vis titration experiments.¹² The values of ΔH° and ΔS° are summarized in Table 4. The experiments were carried out in amylene-containing chloroform. Binding constants in amylene-containing chloroform were identical to those in ethanol-free chloroform. The two-point recognition host **3** shows similar values of ΔH° and ΔS° for Leu-OMe, Asp-OMe, and Glu-OMe. In contrast to this, the values of ΔH° and ΔS° for three-point recognition host **1** change sensitively as the guest structures change. Asp-OMe selectivity observed for host **1** is achieved by the more negative enthalpy change for this guest.

(12) Wilcox et al.^{4g} pointed out that a small amount of water in chloroform has a dramatic effect on the values of ΔH and ΔS of association process through hydrogen bonding. The amount of water in amylene-containing chloroform used in our experiments was less than 2 mM as estimated by NMR integration, indicating that the chloroform is “dry” as compared to their CHCl_3 .

Circular Dichroism Studies of the Binding. The induced CD spectra were recorded under the conditions that more than 90% of the host is complexed with a guest. The split type induced CD was observed for all the amino acid esters examined, including Leu-OMe, Asp-OMe, and Glu-OMe (Table 5, Figure 3). It should be noted that the intensities of the induced CD (ICD) are slightly smaller than those observed for host **3** except for Asp-OMe. This reduction in intensity may be explained by the assumption, suggested by the ^1H NMR titration, that at least two configurations are possible in the host–guest complex, one has hydrogen bonding between (guest)10...2-HO(host) and the other has hydrogen bonding between (guest)10...7-HO(host). Alternatively, the longer distance of the distant carbonyl chromophore (hydrogen bonded to 7-OH) from the porphyrin chromophore than the proximal carbonyl group (hydrogen bonded to 2-OH) may result in the ineffective coupling between the chromophores, leading to diminished contribution from the distant carbonyl group to the induced CD. This can also account for the present induced CD.

Discussion

UV–Vis and NMR Studies of Binding. UV–vis titration of host **1** with amino acid esters indicates that the Soret band of **1** shifted to a long wavelength with several isosbestic points, suggesting a 1:1 complexation with the amino group coordinating to zinc.¹³ ^1H NMR titration also indicates that amino acid esters are close to the central metal of porphyrin host **1** in the complex. For a guest bearing one hydrogen-bonding site, Leu-OMe, both hydroxyl protons of host **1**, 2-OH and 7-OH, shifted downfield (Figure 2a). This observation suggests that both hydroxyl groups, 2-OH and 7-OH, participate in the hydrogen bonding to the guest (Figure 4). The complexation-induced shift (CIS) of the 2-OH proton is larger than that of the 7-OH proton by 43%. For complexation between host **1** and Asp-OMe, where three pairs of interactions are possible, the CIS values of the hydroxyl groups are approximately twice as large as those induced by Leu-OMe (Figure 2b). The CIS values of the 2-OH proton and the 7-OH proton are almost the same. These observations are consistent with the formation of two hydrogen bonds between **1** and Asp-OMe (Figure 5). The CIS value of the 7-OH signal observed for Glu-OMe is similar to that observed for Asp-OMe, while the CIS value of the 2-OH signal for Glu-OMe is smaller than that for Asp-OMe. This result indicates that Glu-OMe is hydrogen bonded to the 7-OH group of host **1** normally and to the 2-OH group in a somewhat distorted fashion. The upfield shift of the naphthyl proton is tentatively ascribed to the shielding effects of the guest carbonyl group because the molecular model indicates that the naphthyl H-8 proton is close to the shielding region of the guest carbonyl group in the host–guest complex.

Induced CD of Amino Acid Ester–Porphyrin Complex. The complex between host **1** and most of the amino acid esters (Table 5) exhibited split type induced CD (ICD) in the Soret region. This characteristic ICD is similar to those observed for the complex between host **3** and amino acid esters, suggesting that these two hosts bind amino acid esters with a similar binding mode. The rotational strengths of the host **1**–amino acid ester complexes are smaller than those of the host **3**–amino acid esters complexes except for Asp-OMe. In previous

(13) Nardo, J. V.; Dawson, J. H. *Inorg. Chim. Acta* **1986**, *123*, 9.

Table 4. Enthalpy and Entropy Changes of the Binding of Amino Acid Esters to Hosts 1, 3 and 6^a

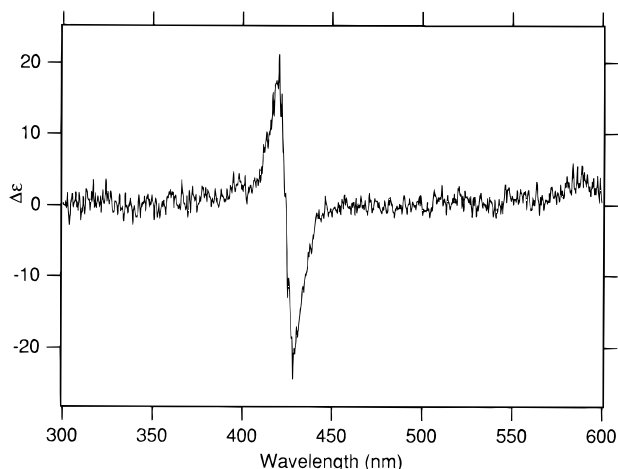
	1		3		6	
	ΔH° (kcal/mol)	ΔS° (cal/K/mol)	ΔH° (kcal/mol)	ΔS° (cal/K/mol)	ΔH° (kcal/mol)	ΔS° (cal/K/mol)
Leu-OMe	-12.5 ± 0.4	-22.7 ± 1.4	-12.4 ± 0.4	-22.7 ± 1.2	-8.3 ± 0.3	-15.4 ± 1.0
Asp-OMe	-14.6 ± 0.5	-26.8 ± 1.6	-11.2 ± 0.5	-21.7 ± 1.5		
Glu-OMe	-13.3 ± 0.5	-24.8 ± 1.3	-11.0 ± 0.4	-21.7 ± 1.3		

^a Determined from the following equation: $R \ln K = -\Delta H^\circ/T + \Delta S^\circ$, where the binding constants (K) were determined by the variable-temperature UV-vis titration experiments between 10 and 40 °C in CHCl_3 containing 0.1% amylene. The plot of $R \ln K$ against $1/T$ was linear, indicating that the differential heat capacity ΔC_p is negligibly small. It was confirmed that the binding constants in amylene-containing CHCl_3 were almost the same as those in ethanol-free CHCl_3 . Ten to fourteen determinations of K were used for the calculation of ΔH° and ΔS° .

Table 5. Rotational Strength (R , 10^{-40} cgs) of CD of Hosts 1 and 3 Induced by Complexation with Amino Acid Esters^a

	1^b				3^c			
	λ_1 (nm)	R_1	λ_2 (nm)	R_2	λ_1 (nm)	R_1	λ_2 (nm)	R_2
Leu-OMe	422.2	25.5	427.7	-25.4	422.2	32.3	427.2	-36.5
Val-OMe	422.3	20.8	427.9	-22.0	424.5	31.5	430.2	-30.2
Ala-OMe	422.8	6.4	431.9	-7.5	424.5	19.2	429.3	-18.0
Phe-OMe	422.1	8.4	428.5	-15.0	422.6	19.0	429.3	-29.9
Trp-OMe	423.2	32.3	427.9	-41.4	423.0	38.2	429.1	-51.4
Pro-OMe	422.3	10.5	430.7	-8.9	422.3	17.6	428.1	-14.2
Glu-OMe	422.4	10.4	430.2	-9.0	422.9	16.1	429.9	-12.5
Asp-OMe	420.2	22.9	427.3	-23.3	424.0	20.6	429.6	-20.3
Glu-OMe ^d	421.1	11.0	425.7	-13.7				
Asp-OMe ^d	421.1	24.0	426.2	-26.9				
Cys-OMe	421.7	6.6	428.9	-9.3				
Met-OMe	422.7	10.8	429.5	-9.6	422.1	10.9	428.1	-13.4

^a In CHCl_3 containing 1% ethanol otherwise noted. ^b At 25 °C. ^c At 15 °C. ^d In CHCl_3 free from ethanol.

**Figure 3.** Induced circular dichroism of a complex prepared from host **1** (3.9×10^{-6} M) and dimethyl aspartate (6.34×10^{-4} M) in chloroform (ethanol free) at 25 °C.

studies,^{2d,14} we reported that the ICD originates from the coupling between the transition moment of the carbonyl chromophore and that of the porphyrin chromophore. From this mechanism, it is predicted that if the two carbonyl groups of Asp-OMe and Glu-OMe are fixed effectively, then the ICD can be doubled or canceled depending on the relative orientation of the carbonyl groups. To discuss the ICD, detailed analysis of the distribution of conformers of host-guest complexes will be necessary.

First, we consider the ICD of the Leu-OMe-**1** complex. Four configurations of the hydrogen-bonding complexes are possible for this complex. For this complex, hydrogen bonding to the 2-OH group (Figure 4, left) and the 7-OH group (Figure 4, right) are the two conformations in which the syn lone pair electrons of the carbonyl group

of the guest participate in the hydrogen bonding. There are two other conformations, in which the anti lone pair electrons are hydrogen bonded. In Figure 4, only the complexes in which the hydroxyl group is hydrogen bonded to the syn lone pair electrons of the carbonyl group are shown. If we consider only the two conformations shown in Figure 4, the transition moments of the carbonyl groups (indicated by arrows in Figure 4) are located in the similar fashion relative to the porphyrin chromophore in both conformations. Therefore ICD should remain unchanged according to the carbonyl-porphyrin coupling mechanism. The observed ICD is slightly reduced in intensity. This observation is consistent with the carbonyl-porphyrin coupling mechanism but suggests that at least one conformation in addition to those shown in Figure 4 also contributes to the present ICD.

The ICD observed for the Asp-OMe-**1** complex is difficult to explain. If we consider the conformation of the Asp-OMe-host **1** complex shown in Figure 6, the transition moments of the two carbonyl groups cancel out; thus a reduced ICD is predicted with respect to that of Leu-OMe-**1** complex. The observed ICD was slightly less intense than that of the Asp-OMe-**3** complex. This may suggest that one or more additional conformations contribute to the ICD of the Asp-OMe-**1** complex. For example, a conformation in which the carbonyl group is almost perpendicular to the porphyrin plane is possible. In this conformation, the coupling between the transition moment of the perpendicular carbonyl group and that of the porphyrin should be very ineffective, and this carbonyl group would then make much less contribution to the ICD. The distance between the carbonyl chromophore and the porphyrin chromophore may be an important factor. Because the carbonyl group hydrogen bonded to the 7-OH group is distant from the porphyrin plane, the coupling between the chromophores is reduced and the contribution to the ICD may be diminished. Alternatively, the three-point fixation may cause the

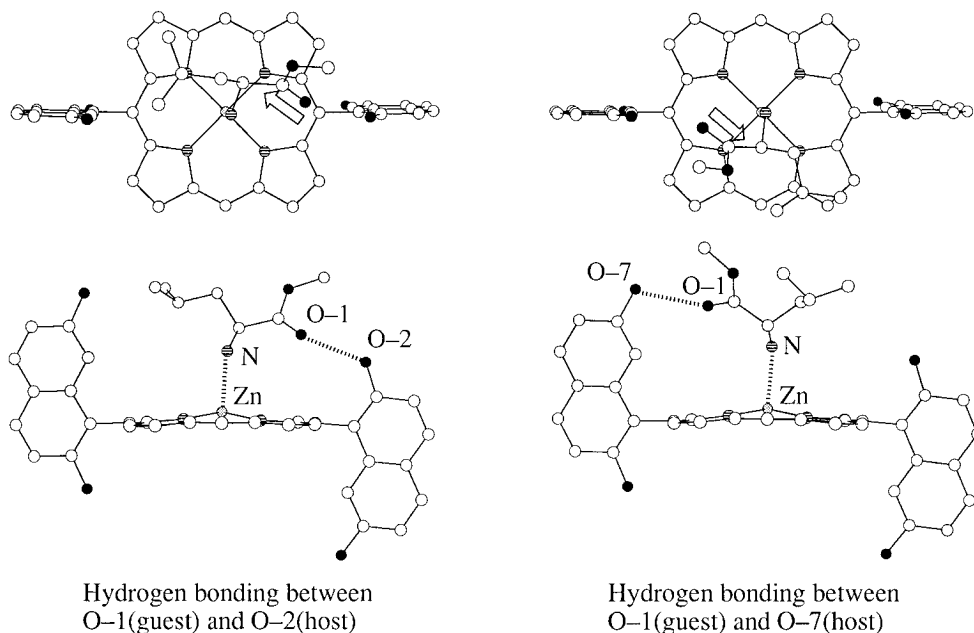


Figure 4. Schematic representation of two conformers of the **1**-Leu-OMe complex. Arrows indicate the direction of the transition dipole moment of the carbonyl group.

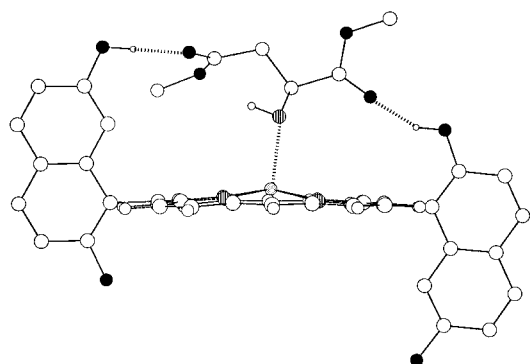


Figure 5. Schematic representation of three-point adduct between **1** and Asp-OMe.

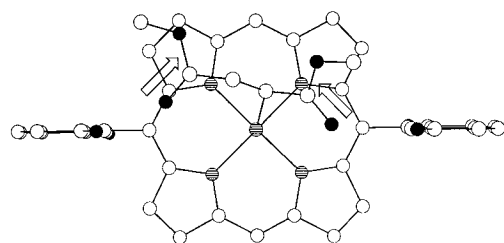


Figure 6. Transition moments of the carbonyl groups in one of possible conformers of the **1**-Asp-OMe complex.

strain in porphyrin framework, resulting in the ICD. Detailed information of the conformation of the host-guest complexes is required to discuss the observed ICD in detail.

Thermodynamic Parameters of Multipoint Recognition. The enthalpy and entropy values of the complexation process indicate that the complexation is enthalpy driven. Table 4 shows that the enthalpy change ($-\Delta H^\circ$) increases as the number of recognition pairs increases except for the difference in the enthalpy changes between the **3**-Leu-OMe complex and the **3**-Asp-OMe complex. Although both of these complexes can have one coordination and one hydrogen-bonding pair, the **3**-Leu-OMe complex is more stable than the **3**-Asp-OMe complex by 1.2 kcal/mol. This result indi-

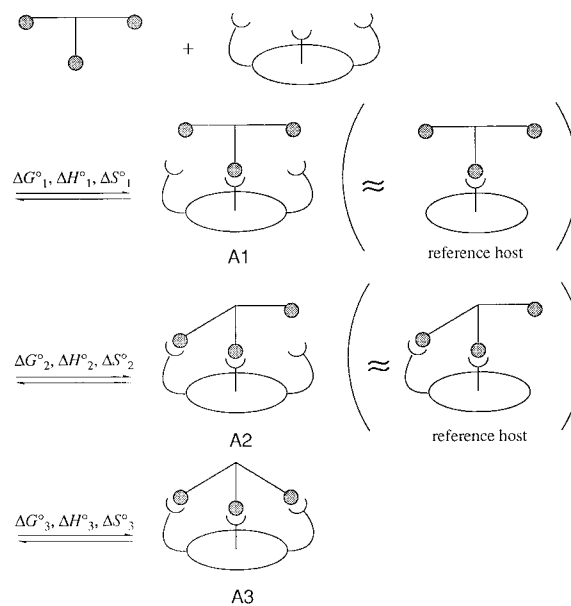


Figure 7. Thermodynamic intermediate states of three-point molecular recognition process. Reference hosts are used to approximate these intermediate states. The reference host-guest complexes are shown in parentheses. A1: hypothetical one-point adduct. A2: hypothetical two-point adduct. A3: three-point adduct. Thermodynamic quantities (ΔG°_i , ΔH°_i , and ΔS°_i , where $i = 1-3$) are determined by reference host or guest.

cates that interactions other than the point-point interaction make a significant contribution to the enthalpy term. In the following discussion, we compare only the complexes consisting of the same guest and different hosts. Enthalpy changes between the complexes consisting of the same guest and different hosts can be reasonably explained in terms of the point-point interaction.

The three-point recognition process was assumed to proceed through a hypothetical one-point adduct and two-point adduct thermodynamic state (Figure 7). The first process (Figure 7, top) is driven by the coordination interaction between the amino group and the zinc ion. In the second process (Figure 7, middle), one hydrogen

Table 6. Coordination and Hydrogen-Bonding Free Energy, Enthalpy, and Entropy in Porphyrin–Amino Acid Multipoint Adducts^a

	free energy, ^b ΔG° , kcal/mol	enthalpy, ΔH° , kcal/mol	entropy, ΔS° , cal/K/mol	compensation temp, ^c °C
coordination (ΔG°_1 , ΔH°_1 , ΔS°_1)	-3.7	-8.3	-15.4	266
hydrogen bond (O1–HO, ΔG°_2 , ΔH°_2 , ΔS°_2)	-1.9	-4.1	-7.3	562
hydrogen bond (O4–HO, ΔG°_3 , ΔH°_3 , ΔS°_3)	-1.5	-3.4	-5.1	666

^a Coordination terms were calculated from the thermodynamic data for complexation of Leu-OMe and host **6**. Hydrogen-bonding (O1–HO) terms were calculated from the difference in thermodynamic data between **3**–Leu-OMe complexation and **6**–Leu-OMe complexation. Hydrogen-bonding (O4–HO) terms were calculated from the difference in thermodynamic data between **1**–Asp-OMe complexation and **3**–Asp-OMe complexation. ^b Free energy was calculated from $\Delta G^\circ_i = \Delta H^\circ_i - T\Delta S^\circ_i$ at 25 °C. ^c The compensation temperature, T_c , was calculated from $T_c = \Delta H^\circ_i / \Delta S^\circ_i$ ($i = 1-3$).

bond forms within the one-point adduct (A1). In the third process (Figure 7, bottom), another hydrogen bond forms to yield the three-point adduct (A3). The values of ΔH°_1 and ΔS°_1 involve the stabilization owing to the coordination interaction and the resulting motional changes (the translational freedom and part of the rotational freedom of guest are lost), respectively. The values of ΔH°_2 and ΔS°_2 involve the stabilization owing to the hydrogen-bonding interaction and the resulting motional changes (the rotational freedom of guest is lost), respectively. The values of ΔH°_3 and ΔS°_3 involve the stabilization owing to the second hydrogen-bonding interaction and the resulting motional changes (the internal rotational freedom of guest is lost), respectively. Thermodynamic quantities of these two hypothetical states were determined by use of reference host **3** and reference host **6**.

The values of ΔG° , ΔH° , and ΔS° for the equilibrium between A0 and A1 and the equilibrium between A1 and A2 are obtained from the thermodynamic parameters determined for Leu-OMe and the following equations.

$$\Delta G^\circ_1 = \Delta G^\circ(\mathbf{6}\text{-Leu-OMe})$$

$$\Delta H^\circ_1 = \Delta H^\circ(\mathbf{6}\text{-Leu-OMe})$$

$$\Delta S^\circ_1 = \Delta S^\circ(\mathbf{6}\text{-Leu-OMe})$$

$$\Delta G^\circ_2 = \Delta G^\circ(\mathbf{3}\text{-Leu-OMe}) - \Delta G^\circ(\mathbf{6}\text{-Leu-OMe})$$

$$\Delta H^\circ_2 = \Delta H^\circ(\mathbf{3}\text{-Leu-OMe}) - \Delta H^\circ(\mathbf{6}\text{-Leu-OMe})$$

$$\Delta S^\circ_2 = \Delta S^\circ(\mathbf{3}\text{-Leu-OMe}) - \Delta S^\circ(\mathbf{6}\text{-Leu-OMe})$$

Similarly, ΔG°_3 , ΔH°_3 , and ΔS°_3 are obtained from the thermodynamic parameters determined for Asp-OMe and the following equations.

$$\Delta G^\circ_3 = \Delta G^\circ(\mathbf{1}\text{-Asp-OMe}) - \Delta G^\circ(\mathbf{3}\text{-Asp-OMe})$$

$$\Delta H^\circ_3 = \Delta H^\circ(\mathbf{1}\text{-Asp-OMe}) - \Delta H^\circ(\mathbf{3}\text{-Asp-OMe})$$

$$\Delta S^\circ_3 = \Delta S^\circ(\mathbf{1}\text{-Asp-OMe}) - \Delta S^\circ(\mathbf{3}\text{-Asp-OMe})$$

These thermodynamic values are listed in Table 6. As the number of recognition pairs increases from one to three, the magnitudes of both ΔH° and ΔS° decrease. This may reflect that the multipoint adduct becomes more ordered as the number of recognition pairs increases.

We can ascribe the ΔS°_3 term primarily to entropy loss owing to the freezing of internal rotation of the guest and the host. The internal rotation along the C2–C3 bond and the C3–C4 bond of Asp-OMe should be restricted together with the C7–O7 bond of the naphthyl group of host. The ΔS°_3 term may also involve a contribution from positive entropy change owing to the desolvation of the

OH group and the C=O group upon binding. Therefore the decrease of entropy owing to the restriction of internal rotation by the second hydrogen bond can be estimated to be larger than 5.1 cal/K/mol. This value is close to the internal rotational entropy along a single bond calculated for Ala-OMe and Val-OMe.¹ The negative enthalpy change owing to one hydrogen bond (ΔH°_3) is 3.4 kcal/mol. This value is also a compensated value by the positive enthalpy change owing to the desolvation of the OH group and the C=O group, namely the stripping of CHCl₃ from these groups. It also involves the changes in conformational energy of guest. Therefore the hydrogen-bonding enthalpy is approximately equal to -3.4 kcal/mol. The hydrogen-bonding energy is reported to be -3.5 to -6.0 kcal/mol for the water dimer in vacuo and the carboxylic acid dimer in a liquid state.¹⁵ The observed hydrogen-bonding enthalpy listed in Table 6 is close to this range.

The compensation temperature¹⁶ for each interaction is also listed in Table 6. The physical meaning of the compensation temperature is as follows. If the temperature of the binding experiment is raised up to the compensation temperature, the attractive interaction will disappear owing to the thermal motion of the molecules. The compensation temperature increases as the number of recognition pairs increases as shown in Table 6. Although the first interaction between zinc and the amino group has large negative ΔH° value, the compensation temperature is not so high. This can be ascribed to the large entropy loss from the restriction of the translational and rotational motion. In contrast, the third interaction, hydrogen bonding between (guest)O4···HO(host), has a much higher compensation temperature of 666 °C. This reflects that the host–guest system is already in an ordered state before the third interaction operates. This trend that the compensation temperature increases as the number of the recognition pairs increases may be the general one in the multipoint molecular recognition.

The selectivity of Asp-OMe over Glu-OMe observed for host **1** is ascribed to the enthalpy change. The enthalpy difference $\Delta\Delta H^\circ$ was 1.3 kcal/mol. To examine the origin of this enthalpy difference, the conformational energy of these guests in the complexed state and the free state was calculated by molecular orbital calculations (the PM3 method).¹⁷ For both of these guests, the coordinates of the host–guest complex were generated so that the coordination interaction and the two hydrogen bonds take place in the complex. The enthalpy change of Asp-OMe from the free form to the complexed form was -0.07 kcal/mol and that of Glu-OMe was +1.6 kcal/mol. Therefore

(15) Jeffrey, G. A.; Saenger, W. *Hydrogen bonding in biological structures*; Springer-Verlag: New York, 1991.

(16) Gelb, R. I.; Schwartz, L. M.; Cardelino, B.; Fuhrman, H. S.; Johnson, R. F.; Laufer, D. A. *J. Am. Chem. Soc.* **1981**, *103*, 1750.

(17) MOPAC Version 5 and Version 6, Stewart, J. J. P. *QCPE Bull.* **1989**, *9*, 10.

Asp-OMe is bound to host **1** via a three-point fixation mode in a stable conformation while Glu-OMe is bound to host **1** in a distorted and unstable conformation. The conformational enthalpy difference can account for the experimentally observed enthalpy difference $\Delta\Delta H^\circ$ of 1.3 kcal/mol.

Experimental Section

General. Dichloromethane, 1,2-dichloroethane, and *N,N*-dimethylformamide were distilled from CaH₂. CHCl₃ used in UV-vis titrations was prepared in one of the following three ways. (1) CHCl₃ free from ethanol: CHCl₃ containing ethanol as a stabilizer (spectrophotometric grade, 99% stabilized with ethanol, Dojindo Laboratories) was washed with distilled water of the same volume three times, dried over anhydrous potassium carbonate, and distilled from CaH₂ under N₂. This CHCl₃ free from ethanol was used for UV-vis titrations within 12 h after distillation. (2) CHCl₃ containing ethanol as a stabilizer: the above spectrophotometric grade CHCl₃ was used as received. (3) CHCl₃ containing amylene as a stabilizer: A.C.S. HPLC grade (99.9% stabilized with amylene, Aldrich) was used as received. Amino acid methyl ester hydrochlorides were commercially available. After neutralization and extraction with dichloromethane, all amino acid esters were freshly distilled just before use for UV-vis titration except for Trp-OMe. Unless otherwise noted, other materials were obtained from commercial sources and used without further purification. Hosts **3** and **6** were prepared by the reported procedure. Because the *cis* and *trans* atropisomers of **6** could not be separated, the mixture was used for the binding constant determination.

Variable-Temperature UV-Vis Spectrophotometric Titration. To (3.8×10^{-6}) – (7.1×10^{-6}) M **1**, **2**, **3**, or **6** in chloroform was added a stock solution of α -amino acid ester in chloroform over the temperature range 10 to 40 °C, and changes in absorbance at 414–416 and 428–430 nm of the Soret band were monitored at eight different concentrations of the guest molecules. The binding constants were calculated assuming 1:1 complexation by use of a computer-assisted nonlinear least-squares method. The concentration of α -amino acid ester was (7×10^{-6}) – (2×10^{-3}) M for host **1**, (3×10^{-5}) – (7×10^{-3}) M for host **2**, (9×10^{-6}) – (4×10^{-3}) M for host **3**, and (6×10^{-4}) – (1.1×10^{-2}) M for host **6**.

The induced CD of the host **1**-amino acid esters was obtained under the conditions that more than 90% of the host is complexed with amino acid esters. The rotational strengths were calculated by fitting the circular dichroism spectra of the 350 to 500 nm region to Gaussian functions: $a_1 \exp(-((\lambda - \lambda_1)/\sigma_1)^2) - a_2 \exp(-((\lambda - \lambda_2)/\sigma_2)^2)$ or $a_1 \exp(-((\lambda - \lambda_1)/\sigma_1)^2)$ where a_1 , a_2 , λ_1 , λ_2 , σ_1 , and σ_2 are parameters to be determined. The rotational strength (R_1 , R_2) was calculated from these parameters. The curve fitting was carried out by use of Igor, WaveMetrics, Inc.

Preparation of 3,4-Diethyl-2-formylpyrrole (7). To DMF (3.96 mL, 5.11 mmol) was added POCl₃ (4.86 mL, 5.21 mmol) dropwise at 0 °C under N₂. After the ice bath was removed, 1,2-dichloroethane (10 mL) was added and the solution was stirred for 20 min. A solution of freshly distilled 3,4-diethylpyrrole¹⁸ (5.9 g, 4.87 mmol) in 1,2-dichloroethane (10 mL) was added, and the resulting solution was heated at 50 °C for 1.5 h. To the brown reaction mixture was added a solution of sodium acetate (5.06 g) in water (39 mL); the reaction mixture was heated again at 80 °C for 40 min. The cooled reaction mixture was extracted with ether, and the organic layer was washed with saturated aqueous Na₂CO₃, water, and saturated aqueous NaCl, dried over anhydrous Na₂CO₃, and evaporated. The residue was recrystallized from hexane to yield 3,4-diethyl-2-formylpyrrole (6.67 g, 90.6%): ¹H NMR (500 MHz, CDCl₃) δ 9.59 (s, 1H), 9.02 (br s, 1H), 6.84 (d, $J = 2.8$ Hz, 1H), 2.72 (q, $J = 7.7$ Hz, 2H), 2.45 (q, $J = 7.7$ Hz, 2H), 1.21 (t, $J = 7.7$ Hz, 3H), 1.19 (t, $J = 7.7$ Hz, 3H); MS m/z 151 (M⁺).

Preparation of 3,3',4,4'-Tetraethyl-2,2'-dipyrrylmethene Hydrobromide (8). To a solution of 3,4-diethylpyrrole (5.34 g, 0.433 mmol) and 3,4-diethyl-2-formylpyrrole (**7**) in ethanol (35 mL, 6.50 g, 0.430 mmol) was added aqueous HBr (47%, 5.5 mL) dropwise at 0 °C. When the reaction mixture turned pale red and precipitates appeared, additional ethanol (10 mL) was added and the solution was stirred well. After 1 h, the solvent was evaporated, and the residue was recrystallized from ethanol to yield 3,3',4,4'-tetraethyl-2,2'-dipyrrylmethene hydrobromide (7.47 g, 42%): ¹H NMR (500 MHz, CDCl₃) 13.24 (br s, 2H), 7.72 (d, $J = 3.7$ Hz, 2H), 7.27 (s, 1H), 2.70 (q, $J = 7.7$ Hz, 4H), 2.48 (q, $J = 7.7$ Hz, 4H), 1.204 (t, $J = 7.7$ Hz, 6H), 1.200 (t, $J = 7.7$ Hz, 6H); FAB MS (3-nitrobenzyl alcohol) m/z 257 (M⁺ - Br).

Preparation of 2,7-Dimethoxynaphthalene (10). A solution of 2,7-dihydroxynaphthalene (500 mg, 3.12 mmol), K₂CO₃ (1.72 g, 12.5 mmol), and CH₃I (0.97 mL, 15.6 mmol) in DMF (3 mL) was heated at 50–60 °C for 3.5 h under N₂. After the reaction mixture was cooled, water was added and the product was extracted with ether. The organic layer was washed subsequently with water and saturated aqueous NaCl, dried over K₂CO₃, filtered, and evaporated to dryness. The residue was recrystallized from ether to yield **10** (270 mg, 46% yield): mp 138 °C; ¹H NMR (500 MHz, CDCl₃) δ 7.65 (d, $J = 8.9$ Hz, 2H), 7.05 (d, $J = 2.5$ Hz, 2H), 6.99 (dd, $J = 2.5, 9.2$ Hz, 2H), 3.90 (s, 6H).

Preparation of 2,7-Dimethoxy-1-naphthaldehyde (11). To a solution of **10** (100 mg, 0.531 mmol) in 1,2-dichloroethane (2 mL) were added *N*-methylformanilide (87 μ L, 0.701 mmol) and POCl₃ (65 μ L, 0.701 mmol). The solution was heated at 100 °C for 11 h. After the mixture was cooled, it was poured into an ice-water mixture. The product was extracted with ether, and the organic layer was washed with 2 M aqueous HCl, dried over Na₂SO₄, filtered, and evaporated. The residue was chromatographed on silica gel column (hexane:ether = 3:1 to 2:1) to obtain **11** (95.4 mg, 83%): mp 101 °C; ¹H NMR (500 MHz, CDCl₃) δ 10.88 (s, 1H), 8.83 (d, $J = 2.8$ Hz, 1H), 7.97 (d, $J = 8.9$ Hz, 1H), 7.65 (d, $J = 8.9$ Hz, 1H), 7.10 (d, $J = 8.9$ Hz, 1H), 7.05 (dd, $J = 2.6, 9.0$ Hz, 1H), 4.03 (s, 3H), 3.96 (s, 3H); IR (KBr) ν_{CO} 1665 cm⁻¹. Anal. Calcd for C₁₃H₁₂O₃: H, 5.59; C 72.21. Found: H, 5.75; C, 72.02.

Preparation of 2-Hydroxy-7-methoxy-1-naphthaldehyde (12). To a solution of **11** (1.20 g, 5.55 mmol) in CH₂Cl₂ (50 mL) cooled to -55 °C was gradually added a solution of BBr₃ in CH₂Cl₂ (1 M, 8.0 mL, 8.0 mmol) under N₂. The reaction mixture was warmed up to room temperature. After 4.5 h, aqueous HCl was added at 0 °C until orange precipitates were dissolved. The product was extracted with ether, and the organic layer was washed with saturated aqueous NaCl, dried over Na₂SO₄, filtered, and concentrated in vacuo. The residue was purified by column chromatography on silica gel (hexane:ether = 4:1 to 1:1) to obtain **12** (0.91 g, 81%): mp 130 °C; ¹H NMR (500 MHz, CDCl₃) δ 13.17 (s, 1H), 10.75 (s, 1H), 7.89 (d, $J = 8.9$ Hz, 1H), 7.70 (d, $J = 8.9$ Hz, 1H), 7.67 (d, $J = 2.5$ Hz, 1H), 7.08 (dd, $J = 8.9, 2.5$ Hz, 1H), 6.98 (d, $J = 8.9$ Hz, 1H), 3.96 (s, 3H); IR (KBr) ν_{CO} 1624 cm⁻¹. Anal. Calcd for C₁₂H₁₀O₃: H, 4.98; C, 71.28. Found: H, 4.98; C, 71.22.

Preparation of *trans*- and *cis*-5,15-Bis(2-hydroxy-7-methoxy-1-naphthyl)-2,3,7,8,12,13,17,18-octaethylporphyrin. To a solution of 3,3',4,4'-tetraethyl-2,2'-dipyrrylmethene hydrobromide (2.70 g, 8.00 mmol) in ethanol (50 mL) was slowly added under N₂ a solution of NaBH₄ (426 mg, 11.26 mmol) in ethanol (15 mL) until the reaction mixture turned from dark brown to pale brown. After stirring for 1 h at room temperature, the solvent was evaporated and to the residue was added ether. The precipitate was filtered off and the filtrate was evaporated to quantitatively yield 3,3',4,4'-tetraethyl-2,2'-dipyrrylmethane (**9**). The dipyrromethane was dissolved in methanol (20 mL, degassed by N₂ bubbling for 1 h), and a solution of **12** (1.60 g, 7.91 mmol) and *p*-toluenesulfonic acid monohydrate (0.39 g, 2.08 mmol) in methanol (105 mL) was added dropwise. After the addition the reaction mixture was stirred for 15 h in the dark. The solvent was evaporated, and the residue was dissolved in THF (168 mL), followed by the addition of chloranil (446 mg, 1.81 mmol). The solution was stirred for 3 h. After the solvent was evaporated, the residue was chromatographed on silica gel column (CHCl₃:

(18) Whitlock, H. W.; Hanauer, R. *J. Org. Chem.* **1968**, *33*, 2169.

AcOEt = 20:1) to separate the trans and the cis isomers. Both isomers were recrystallized from CHCl₃–hexane: Trans isomer, $R_f = 0.59$ (CHCl₃:AcOEt = 20:1); cis isomer, $R_f = 0.21$ (CHCl₃:AcOEt = 20:1). Since the trans isomer was contaminated with an impurity having the same R_f value, it was converted to a zinc complex and purified by silica gel column chromatography (CHCl₃) and recrystallized from CHCl₃–hexane.

Trans Isomer Zinc Complex 2. To the crude trans isomer (400 mg) dissolved in CHCl₃ (150 mL) was added methanol saturated with zinc acetate (30 mL), and the solution was refluxed for 2 h. Water was added to the reaction mixture, the organic layer was separated, and the aqueous layer was extracted with CHCl₃. The combined organic layer was dried over Na₂SO₄ and evaporated in vacuo. The residue was purified by silica gel column chromatography (CHCl₃). Further purification by recrystallization from CHCl₃–hexane afforded pure **2** (red purple powder; 172 mg, first crop) followed by a second crop of 234 mg (total yield 406 mg, 10.9% based on dipyrromethene): reddish purple powder, mp > 300 °C dec; UV–vis (CHCl₃ containing amylene) λ_{\max} (log ϵ) 416 (5.47), 542 (4.29), 578 (4.24); ¹H NMR (500 MHz, CDCl₃) 10.23 (s, 2H), 8.20 (d, $J = 9.0$ Hz, 2H), 7.95 (d, $J = 9.2$ Hz, 2H), 7.46 (d, $J = 9.0$ Hz, 2H), 7.01 (dd, $J = 9.0, 2.6$ Hz, 2H), 6.05 (d, $J = 2.6$ Hz, 2H), 5.14 (s, 2H), 4.00–3.93 (m, 4H), 2.86–2.78 (m, 4H), 2.78 (s, 6H), 2.60–2.52 (m, 4H), 1.85 (t, $J = 7.7$ Hz, 12H), 0.93 (t, $J = 7.6$ Hz, 12H); HRMS calcd for C₅₈H₆₀O₄N₄Zn 940.391, found 940.391.

Cis isomer free base 13: yield 214 mg, 6.1%; purple crystal, mp > 300 °C dec; UV–vis (CHCl₃ containing amylene) λ_{\max} (log ϵ) 414 (5.21), 512 (4.00), 544 (3.79), 578 (3.77), 628 (3.44); ¹H NMR (500 MHz, CDCl₃) 10.33 (s, 2H), 8.19 (d, $J = 8.9$ Hz, 2H), 7.96 (d, $J = 9.2$ Hz, 2H), 7.45 (d, $J = 9.2$ Hz, 2H), 7.04 (dd, $J = 8.9, 2.8$ Hz, 2H), 6.22 (d, $J = 2.5$ Hz, 2H), 5.15 (s, 2H), 4.00–3.94 (m, 8H), 2.90–2.82 (m, 4H), 2.85 (s, 6H), 2.70–2.62 (m, 4H), 1.85 (t, $J = 7.6$ Hz, 12H), 0.97 (t, $J = 7.5$ Hz, 12H), –1.70 (br, 2H); HRMS calcd for C₅₈H₆₂O₄N₄ 878.477, found 878.481.

Preparation of trans-5,15-bis(2-hydroxy-7-methoxy-1-naphthyl)-2,3,7,8,12,13,17,18-octaethylporphyrin (14): mp > 300 °C dec; UV–vis (CHCl₃ containing amylene) λ_{\max} (log ϵ) 414 (5.22), 512 (4.19), 544 (3.83), 578 (3.82), 628 (3.53); ¹H NMR (500 MHz, CDCl₃) 10.32 (s, 2H), 8.19 (d, $J = 8.9$ Hz, 2H), 7.95 (d, $J = 8.9$ Hz, 2H), 7.45 (d, $J = 8.9$ Hz, 2H), 7.02 (dd, $J = 9.2, 2.5$ Hz, 2H), 6.12 (d, $J = 2.5$ Hz, 2H), 5.10 (s, 2H), 4.14–3.92 (m, 8H), 2.92–2.82 (m, 4H), 2.79 (s, 6H), 2.70–2.60 (m, 4H), 1.83 (t, $J = 7.6$ Hz, 12H), 0.97 (t, $J = 7.5$ Hz, 12H), –1.83 (br, 2H); HRMS calcd for C₅₈H₆₂O₄N₄ 878.477, found 878.482.

Preparation of trans-5,15-Bis(2,7-dihydroxy-1-naphthyl)-2,3,7,8,12,13,17,18-octaethylporphyrin (15). Since **2** is nearly insoluble in CH₂Cl₂, **2** (22.9 mg, 24.3 μ mol) was demetallated by the addition of 3 M aqueous HCl followed by the treatment with saturated aqueous NaHCO₃ to obtain the free base. To the free base dissolved in CH₂Cl₂ (15 mL) and cooled to –70 °C was added a solution of BBr₃ in CH₂Cl₂ (1 M, 0.58 mL) slowly. After the reaction mixture was allowed to warm to room temperature over 3 h, excess BBr₃ was decomposed by the addition of MeOH. To the solution was added saturated aqueous NaHCO₃, the resultant mixture was extracted with CH₂Cl₂, dried over Na₂SO₄, and filtered, and the solvent was evaporated. The residue was purified by column chromatography on silica gel (CHCl₃:AcOEt = 10:1), and recrystallized from hexane–CHCl₃ to obtain the free base of **1** (7.3 mg, 35%, purple powder): mp > 300 °C dec; UV–vis (CHCl₃ containing amylene) λ_{\max} (log ϵ) 414 (5.31), 512 (4.30), 546 (3.99), 578 (3.95), 628 (3.70); ¹H NMR (500 MHz, CDCl₃) 10.31 (s, 2H), 8.18 (d, $J = 8.9$ Hz, 2H), 7.95 (d, $J = 8.9$ Hz, 2H), 7.46 (d, $J = 8.9$ Hz, 2H), 6.96 (dd, $J = 8.9, 2.5$ Hz, 2H), 5.97 (d, $J = 2.5$ Hz, 2H), 5.22 (s, 2H), 4.83 (br, 2H), 4.03–3.93 (m, 8H), 2.95–2.86 (m, 4H), 2.68–2.59 (m, 4H), 1.84 (t, $J = 7.7$ Hz, 12H), 0.99 (t, $J = 7.5$ Hz, 12H), –1.81 (br, 2H); HRMS calcd for C₅₆H₅₈O₄N₄ 850.446, found 850.453.

Preparation of [trans-5,15-Bis(2,7-dihydroxy-1-naphthyl)-2,3,7,8,12,13,17,18-octaethylporphyrinato]zinc(II) (1). Zinc was inserted by using the same procedure as that used for **2**. The zinc complex was purified by silica gel column

chromatography (CHCl₃:AcOEt = 10:1) and recrystallized from CHCl₃–hexane to yield **1** in quantitative yield: mp > 300 °C dec; UV–vis (CHCl₃ containing amylene) λ_{\max} (log ϵ) 416 (5.45), 542 (4.28), 578 (4.23); ¹H NMR (500 MHz, CDCl₃) 10.22 (s, 2H), 8.19 (d, $J = 9.1$ Hz, 2H), 7.94 (d, $J = 9.1$ Hz, 2H), 7.46 (d, $J = 8.8$ Hz, 2H), 6.95 (dd, $J = 8.8, 2.4$ Hz, 2H), 5.94 (d, $J = 2.4$ Hz, 2H), 5.20 (s, 2H), 4.17 (s, 2H), 4.03–3.91 (m, 8H), 2.91–2.83 (m, 4H), 2.64–2.55 (m, 4H), 1.84 (t, $J = 7.7$ Hz, 12H), 0.94 (t, $J = 7.5$ Hz, 12H); HRMS calcd for C₅₆H₅₆O₄N₄Zn 912.359, found 912.368.

Preparation of cis-5,15-Bis(2,7-dihydroxy-1-naphthyl)-2,3,7,8,12,13,17,18-octaethylporphyrin (17). The methoxy groups of **13** (37.7 mg, 40.0 μ mol) were deprotected to hydroxy groups by using the same procedure as that for **15**. The cis isomer was purified by silica gel column chromatography (CHCl₃:AcOEt = 10:1) and recrystallized from CHCl₃–hexane to obtain **17** (28.3 mg, 83%, purple powder): mp > 300 °C dec; UV–vis (CHCl₃ containing amylene) λ_{\max} (log ϵ) 414 (5.23), 510 (4.20), 546 (3.88), 576 (3.87), 628 (3.58); ¹H NMR (500 MHz, CDCl₃) 10.30 (s, 2H), 8.18 (d, $J = 8.8$ Hz, 2H), 7.95 (d, $J = 9.1$ Hz, 2H), 7.45 (d, $J = 9.0$ Hz, 2H), 6.96 (dd, $J = 8.9, 2.5$ Hz, 2H), 5.97 (d, $J = 2.1$ Hz, 2H), 5.24 (br, 2H), 4.21 (br, 2H), 4.05–4.10 (m, 8H), 2.96–2.86 (m, 4H), 2.64–2.60 (m, 4H), 1.84 (t, $J = 7.7$ Hz, 12H), 0.98 (t, $J = 7.5$ Hz, 12H), NH (not observed for broadening); HRMS calcd for C₅₆H₅₈O₄N₄ 850.446, found 850.451.

Preparation of [cis-5,15-Bis(2,7-dihydroxy-1-naphthyl)-2,3,7,8,12,13,17,18-octaethylporphyrinato]zinc(II) (4). Zinc was inserted to **17** (18.7 mg, 22.0 μ mol) by using the same procedure as that used for **2**. The zinc complex was purified by silica gel column chromatography (CHCl₃:AcOEt = 5:1) and recrystallized from CHCl₃–hexane to obtain **4** (14.0 mg, 70%, reddish purple powder): mp > 300 °C dec; UV–vis (CHCl₃ containing amylene) λ_{\max} (log ϵ) 416 (5.47), 542 (4.27), 578 (4.23); ¹H NMR (500 MHz, CDCl₃) 10.22 (s, 2H), 8.19 (d, $J = 8.9$ Hz, 2H), 7.95 (d, $J = 8.8$ Hz, 2H), 7.47 (d, $J = 9.2$ Hz, 2H), 6.94 (dd, $J = 8.9, 2.7$ Hz, 2H), 5.86 (d, $J = 2.5$ Hz, 2H), 5.27 (s, 2H), 4.12 (s, 2H), 4.02–3.88 (m, 8H), 2.80–2.91 (m, 4H), 2.50–2.62 (m, 4H), 1.84 (t, $J = 7.7$ Hz, 12H), 0.95 (t, $J = 7.5$ Hz, 12H); HRMS calcd for C₅₆H₅₆N₄O₄Zn 912.359, found 912.354.

Preparation of Bridged Porphyrin 16. To a solution of cis-5,15-bis(2-hydroxy-7-methoxy-1-naphthyl)-2,3,7,8,12,13,17,18-octaethylporphyrin (**13**) (30 mg, 34.1 μ mol) in acetone (120 mL) was added 1,8-dibromooctane (9.28 mg, 34.1 μ mol), and the solution was refluxed for 1 week. After the solvent was removed by evaporation, water was added to the residue and the mixture was extracted with ether. Purification by chromatography on silica gel (hexane:AcOEt = 20:1) and recrystallization from CHCl₃–hexane afforded the bridged porphyrin **16** (6.0 mg, 18.1%, purple crystal): mp > 300 °C dec; UV–vis (CHCl₃ containing amylene) λ_{\max} 418, 513, 546, 582, 635; ¹H NMR (500 MHz, CDCl₃) 10.16 (s, 2H), 8.15 (d, $J = 8.9$ Hz, 2H), 8.03 (d, $J = 9.2$ Hz, 2H), 7.62 (d, $J = 2.1$ Hz, 2H), 7.23–7.19 (m, 2H), 4.00–3.90 (m, 4H), 3.34 (s, 6H), 3.24 (t, $J = 5.5$ Hz, 4H), 2.85–2.76 (m, 4H), 2.65–2.55 (m, 4H), 1.83 (t, $J = 7.6$ Hz, 12H), 0.83 (t, $J = 7.5$ Hz, 12H), –0.39 to –0.47 (m, 4H), –1.60 (br, 2H), –1.68 to –1.76 (m, 4H), –2.25 to –2.32 (m, 4H); HRMS calcd for C₆₆H₇₆O₄N₄ 988.587, found 988.595.

Acknowledgment. We thank T. Kobatake for his kind help in the mass spectroscopy measurements. This work was supported by a Grant-in Aid for Scientific Research (No. 06650980, No. 04101003) from the Ministry of Education, Science, and Culture of Japan.

Supporting Information Available: ¹H NMR spectra for compounds **1**, **2**, **4**, **7**, **8**, **13**, **15**, **16**, and **17** (9 pages). This material is contained in libraries on microfiche, immediately follows this article in the microfilm version of the journal, and can be ordered from the ACS; see any current masthead page for ordering information.